

Fault Diagnosis of Generalized n -Levels 3-phase CHB Multilevel Converters

K.O. Mtepele, D.U. Campos-Delgado, J.A. Pecina-Sánchez,
A.A. Valdez-Fernández, P.R. Martínez-Rodríguez

*Facultad de Ciencias, Universidad Autónoma de San Luis Potosí, San
Luis Potosí, México (e-mail: mtepele@fc.uaslp.mx,
ducd@fciencias.uaslp.mx, angel.pecina@alumnos.uaslp.edu.mx,
andres.valdez@ieee.org, pamartinez@ieee.org)*

Abstract: This paper aims to expand the definition of a comprehensive model-based fault diagnosis strategy for open-circuit faults (OCFs) in the switching devices of a cascaded H-bridge converter with n -levels (CHB- n L), so that it can be used in 3-phase systems. Thereby the application of the CHB- n L converter as a 3-phase active filter is the objective of this work. The OCFs are modeled as additive profiles into the subsystems describing the dynamics of each H-bridge in the converter, where each fault profile is identified by a constant component plus an oscillatory term. The diagnosis task is performed by suggesting a nonlinear sliding-mode proportional-integral (PI) observer to estimate the above profiles, independently of the operating point of the converter. Based on the estimated constant components, fault detection and isolation is achieved without the necessity of additional sensors besides the ones usually used for control purposes. The proposed diagnosis scheme is validated in simulation under single and simultaneous fault scenarios.

Keywords: Fault diagnosis, open-circuit faults, multilevel converter, sliding-mode observer.

1. INTRODUCTION

The growing number of nonlinear loads connected to the grid has produced a negative impact on the quality of electric power supply; Harmonic produced by electrical equipment, such as computers, communication equipments and electronic lighting ballasts, etc; because of the economic cost in the design process, the magnetization curve of the iron core is in the nonlinear saturation state. Consequently, these harmonics increase power losses, deteriorate the quality of the voltage waveform, mislead metering devices, and may cause resonance and interferences. Thus, active power filters (APFs), which operate as controllable power sources with fast transient response, are aimed to compensate reactive power and eliminate harmonics. The APF suppresses the source harmonic current by canceling the harmonic current which is out-of-phase from the load harmonic currents. The principle APF is to detect the source load harmonic currents, to use proper control strategy to inject harmonic currents to mitigate the source harmonic currents (Valdez et al., 2013).

In industrial applications and alternative energy systems, cascaded H-bridge (CHB) multilevel converters are used to construct APFs. These converters have been studied due to their scalability, feasibility, reliability and modularity (Marks et al., 2014)-(Townsend et al., 2016). A series connection of single-phase H-bridge converters with separated DC buses is employed in a CHB multilevel converter. However, both an adequate modulation algorithm and a control strategy must be jointly applied to correctly exploit the advantages of CHB multilevel converters. In which, a good knowledge of a mathematical model of the

system dynamics is a key step for a successful application (Kouro et al., 2011). This dynamic model can be further employed in a model-based fault detection and isolation (FDI) strategy of the CHB multilevel converter (Isermann, 2006).

In this context, novel APF rely on the advantages of multilevel topologies to achieve a high performance, but at the expense of a large number of semiconductor devices. Nonetheless, the probability of a fault in multilevel converters is raised by the number of semiconductors employed in the topology (Mirafzal, 2014). In (Choi et al., 2015) and many other literatures, it has been documented that a high percentage of faults occurs in the switching devices of the multilevel converters, which can be classified in two groups: open-circuit faults (OCFs), and short-circuit ones (SCFs). However, under appropriate passive protections in the power converter topology, these two classes can have the same electrical symptoms and can be treated with similar diagnostic algorithms (Wang et al., 2015). Thus, there is a great interest on detecting and isolating the above mentioned common power device faults that could occur in semiconductor power devices of multilevel converter. In addition, the diagnostic results can help reduce the downtime cost of industrial power electronics systems. More importantly, the information on the identified faulty switches in multilevel converters can be utilized to trigger the corresponding fault-tolerant operation strategy for safety-critical applications (ZhendongJi et al., 2014).

On the subject of OC fault diagnosis, many solutions have been proposed Mirafzal (2014) - (Ouni et al., 2015).

Specifically, Mirafzal (2014) gives a detailed review of published fault detection techniques, while Choi et al. (2015) provides an overview of the failure mechanisms in IGBTs modules and their handling methods. Meanwhile, a fault diagnosis and fault tolerant method for SCF in cascaded half-bridge inverters based on a model-based approach was suggested by Alavi et al. (2015). In (Ouni et al., 2015), a method to detect the faulty cell in a CHB inverter is proposed by comparing the output voltage with the reference one synthesized by the control states of the switches and DC-link voltage.

Voltage-based techniques developed and proposed in (Shu et al., 2016) allow fast detection time and good performance. But they require using additional sensors, which increase the system complexity and cost. More recently, the observer-based methods have been proposed for FDI purposes. Different types of current observers such as Luenberger state observer, nonlinear observers, or proportional integral observers are employed. We rely on these methods because they perform good diagnosis with relatively short detection time, which is very important factor (An et al., 2016) - (Jlassi et al., 2016).

In this context, this research work stands as an extension to our previous effort in (Mtepele et al., 2016) and (Mtepele et al., 2016), thereby the FDI strategies for the single-phase CHB converter was addressed. In the present work, the latter FDI approaches are expanded to adapt the 3-phase CHB converters. To achieve these goals, the CHB- nL converter as a shunt APF is studied, and as a consequence, the generalized model for the whole system is obtained. Later on we base on the system description to model the OCFs as additive signals into each subsystem of the multilevel converter. The dynamic structure of the mode suggests the use of a global proportional-integral (PI) observer per phase to detect and isolate the OCFs by using a sliding-mode philosophy. In order to validate the technique, simulation evaluation under a closed-loop operation of the shunt APF is conducted.

The rest of the paper is organized in the following mode. Section 2 provides a briefly description of the 3-phase CHB- nL converter used in this work. Also, it introduces the mathematical model and the control philosophy for the shunt APF operation. The fault modeling for OCFs, the residual generation based on sliding-mode PI nonlinear observers, and the proposed fault detection and isolation schemes are detailed in Section 3. In Section 4, the simulation evaluation of the new FDI scheme is illustrated based on a 3-phase CHB topology of seven-levels, and finally concluding remarks are described in Section 5.

2. CHB CONVERTER PROPOSED MODEL

Figure 1 shows the general structure of the studied 3-phase CHB- nL converter topology used as shunt APF in this research work. The generalized model of the system represented in Fig. 1 can be obtained by the application of Kirchhoff's law. This procedure yields the following average model of the system dynamics,

$$i_{Sp} = i_p + i_{0p} \quad (1)$$

$$L \frac{d}{dt} i_p = v_{Sp} - \sum_{j=1}^N u_{pj} v_{Cpj} + v_{n0}, \quad (2)$$

$$C \dot{v}_{Cpj} = u_j i_p - \frac{1}{R} v_{Cpj} \quad (3)$$

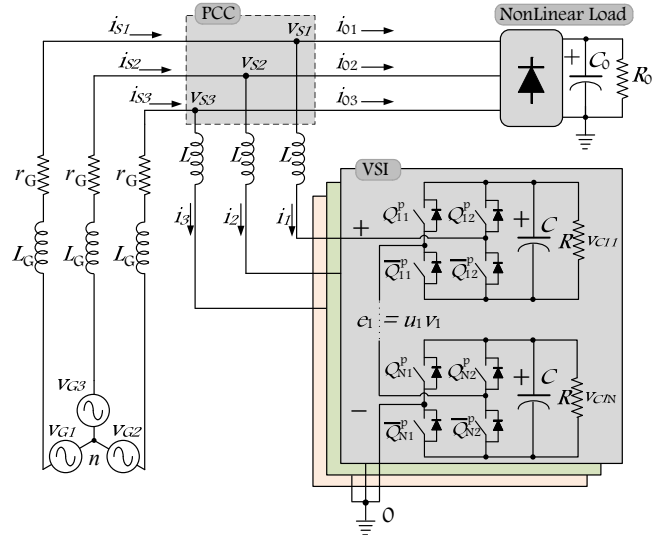


Fig. 1. Three-phase CHB- nL converter used as shunt APF.

where $p \in \{1, 2, 3\}$, $j \in \{1, \dots, N\}$, v_{Sp} denotes the voltage at the point of common coupling (PCC) per phase p , also referred as the grid voltage, i_{Sp} is the phase grid current, i_p is the phase injected current, i_{0p} is the distorted load current consumed by the nonlinear load (NLL); v_{Cpj} is the capacitor voltage in the DC bus of the j -th H-bridge, and $u_{pj} \in [-1, 1]$ the corresponding duty cycle. Parameter L is the input inductor per phase of the shunt APF, C is the capacitance in the DC buses, and R is the resistor that models the losses in each H-bridge. For more details on the mathematical modeling, the reader may refer to (Valdez et al., 2015).

Based on the structure of the previous generalized model, a nominal controller was presented in Valdez et al. (2015), and for completeness is briefly outlined in this work. This controller consists of three feedback loops: a current tracking loop, a voltage regulation loop and $N - 1$ voltage balance loops. The first one was composed of a damping term plus a bank of harmonic oscillators tuned at the harmonics of interest. The voltage regulation loop consisted of a conventional PI controller with limited bandwidth, so that the DC buses in the H-bridges are fixed, in average, at a constant value V_d . To achieve voltage balancing, $N - 1$ control laws are synthesized as amplitude-modulated signals proportional to the fundamental component of the grid voltage, where the modulating gains are obtained by conventional PI control laws. A current reference proportional to the fundamental component of the grid voltage was used to guarantee an almost pure sinusoidal grid current. Following the similar procedures to the single-phase case presented in (Mtepele et al., 2016), the injected currents i_p , and the DC link voltages v_{Cpj} are assumed to be known variables available for both control and fault diagnosis purposes (Valdez et al., 2015).

3. FAULT DIAGNOSIS

The model described by (2) is employed for the synthesis of the dedicated sliding-mode observers in the model-based FDI proposal. Therefore, these observers are used for the detection and isolation of the OCFs in the switching devices of the CHB- n L converter. For this purpose, only the measurements of the injected current i_p and capacitor voltages v_{Cpj} are necessary to implement the diagnosis media.

3.1 Fault Modeling in the CHB- n L Converter

In (Mtepele et al., 2016), the authors addressed that once an OCF scenario occurs, the effect of this fault is suddenly reflected in the performance and efficiency of the CHB- n L converter, which is directly associated with a reduction of its voltage gain. This consideration allows to model the converter faults by using an additive structure (Pecina et al., 2013). In this way, the j -th faulty actuator signal of p -th phase $u_{pj}^f(t)$ is modeled as

$$u_{pj}^f(t) = u_{pj}(t) + f_{pj}(t) \quad (4)$$

where $p \in \{1, 2, 3\}$, $j \in \{1, \dots, N\}$, $f_{pj}(t)$ represents the induced fault profile in the j -th H-bridge of p -th phase. When the OCF occurs in the switching devices Q_{1j}^p or/and \bar{Q}_{2j}^p , the j -th H-bridge of p -th phase is not able to supply the positive state of the output voltage $u_{pj}v_{Cpj}$. This leads to a fault profile f_{pj} that exhibits a negative direction, i.e. $f_{pj} < 0$. On the other hand, when the OCF occurs in switches \bar{Q}_{1j}^p or/and Q_{2j}^p , now the j -th H-bridge of p -th phase is not able to supply the negative state of the output voltage. As a result, the positive profile is induced by this type of fault, i.e. $f_{pj} > 0$.

Similarly to the analysis performed in Pecina et al. (2013) and due the switching strategy in the CHB- n L converter, the pattern described by the j -th faulty actuator of p -th phase $u_{pj}^f(t)$ must be periodic, and as a consequence, it presents a DC component plus harmonic components of the fundamental frequency in the converter. In fact, the DC component will be a distinctive characteristic of the OCFs present in the converter. Therefore the total fault profile induced by the j -th faulty H-bridge of p -th phase can be expressed as

$$f_{pj}(t) = f_{pj}^{DC} + f_{pj}^{OSC}(t), \quad (5)$$

where $p \in \{1, 2, 3\}$, $j \in \{1, \dots, N\}$, f_{pj}^{DC} denotes the DC term and $f_{pj}^{OSC}(t)$ is the oscillatory component. Hence the proposed FDI scheme can be focused just on evaluating f_{pj}^{DC} for the next following reasoning:

Fault Detection: A fault will induce an asymmetric actuator signal where $f_{pj}^{DC} \neq 0$,

Fault Isolation: The faulty pair of switches in the H-bridge can be isolated by the pattern: (i) $(Q_{1j}^p, \bar{Q}_{2j}^p)$ if $f_{pj}^{DC} < 0$, and (ii) $(\bar{Q}_{1j}^p, Q_{2j}^p)$ if $f_{pj}^{DC} > 0$.

In fact, due to the structure of CHB- n L converters, the oscillatory components in the fault profiles $f_{pj}(t)$ are always bounded signals, i.e. $\exists \Gamma > 0$ such that $|f_{pj}^{OSC}(t)| < \Gamma \forall t, j$.

3.2 Residual Generation by Model-Based Approach

As described earlier, the proposed FDI scheme for OCFs relies on a model-based approach through dynamic observer design. In the literature, several approaches have been proposed for system observation (Isermann, 2006). The PI observer is one of the dynamical structures for state observation widely used due to their simplicity and capability to reject or estimate certain perturbations (Perruquetti and Barbot, 2002). Consequently, the dynamic structure of the PI observer is suggested to reconstruct the state dynamics and generate an estimation of the fault profiles. From (2) and (3), the faulty model of shunt APF can be expressed as

$$\begin{aligned} L \frac{d}{dt} i_p &= v_{Sp} - \sum_{j=1}^N (u_{pj} + f_{pj}) v_{Cpj} + v_{n0}, \\ C \dot{v}_{Cpj} &= (u_{pj} + f_{pj}) i_p - \frac{1}{R} v_{Cpj}, \end{aligned} \quad (6)$$

where $p \in \{1, 2, 3\}$, $j \in \{1, \dots, N\}$. From the previous model and as expected, j -th faulty actuator p -th phase $u_{pj}^f(t)$ modifies the overall injected current i_p dynamics, as well as, the capacitor voltage time profile for its H-bridge. Hence, the fault profile generates coupling among the injected current and capacitor voltage dynamics in the shunt APF. For this reason, we suggest proposing to build a global sliding-mode PI nonlinear observer for the states and the fault profiles estimation of p -th phase, based only on the information from the capacitor voltages v_{Cpj} and the injected current i_p , i.e., extra measurements (sensors) are not necessary at all.

Proposition: The dynamical structure of the global sliding-mode PI nonlinear observer in p -th phase for FDI purposes is conformed by a copy of each subsystem in (6) plus linear and nonlinear correction terms, and an augmented state \hat{f}_{pj} to ensure the estimation of the DC fault profile:

$$\begin{aligned} L \frac{d}{dt} \hat{i}_p &= v_{Sp} - \sum_{j=1}^N (u_{pj} + \hat{f}_{pj}) v_{Cpj} + K_i (i_p - \hat{i}_p) \\ &\quad + M_i |i_p - \hat{i}_p|^2 \text{sign}(i_p - \hat{i}_p) + v_{n0}, \\ C \dot{\hat{v}}_{Cpj} &= -\frac{1}{R} \hat{v}_{Cpj} + (u_{pj} + \hat{f}_{pj}) i_p + K_v (v_{Cpj} - \hat{v}_{Cpj}) \\ &\quad + M_v |v_{Cpj} - \hat{v}_{Cpj}|^2 \text{sign}(v_{Cpj} - \hat{v}_{Cpj}), \\ \dot{\hat{f}}_{pj} &= K_f \left[i_p (v_{Cpj} - \hat{v}_{Cpj}) - v_{Cpj} (i_p - \hat{i}_p) \right] \end{aligned} \quad (7)$$

where $p \in \{1, 2, 3\}$, $j \in \{1, \dots, N\}$, for simplicity the positive gains $(K_i, M_i, K_v, M_v, K_f)$ are equivalent to all observers and $K_f > 0$ affects the desired convergence rate of the estimation. With these observers, the estimation errors in the injected current and capacitor voltages are bounded to a neighborhood of the origin, and the error in the DC fault profile is also bounded. The convergence proof of these estimation errors (in a single-phase converter) was detailed in (Mtepele et al., 2016). In this way, similar conclusions are reached when following procedures shown in the above reference. From these conclusions the following tuning condition for the observer gains K_v is needed

$$K_v + \frac{1}{R} > 0. \quad (8)$$

Furthermore, the control gains M_i and M_v in the sliding-mode correction terms affect the upper bounds of the current and voltage estimation errors.

3.3 Fault Detection and Isolation

From the sliding-mode PI nonlinear observers in (7), the DC components of the fault profiles f_{pj}^{DC} are estimated by \hat{f}_{pj} . Due to the rapid variations of the injected current i_p with $p \in \{1, 2, 3\}$ (Valdez et al., 2015), the estimations \hat{f}_{pj} may present oscillatory components, so in order to obtain a pure DC term, from the estimated total fault profile \hat{f}_{pj} , the following moving average is calculated

$$\hat{f}_{pj}^{DC}(t) = \frac{1}{T} \int_{t-T}^t \hat{f}_{pj}(\tau) d\tau. \quad (9)$$

where $p \in \{1, 2, 3\}$, $j \in \{1, \dots, N\}$, T period of the supply voltage v_{Sp} . Next, following the discussion in Section 3.2, the residuals r_{pj} are formulated by taking into account the uncertainty in the estimations as

$$r_{pj} = \begin{cases} 1, & |\hat{f}_{pj}^{DC}| > J_{TH} \\ 0, & |\hat{f}_{pj}^{DC}| \leq J_{TH} \end{cases} \quad (10)$$

with $p \in \{1, 2, 3\}$, $j \in \{1, \dots, N\}$, where the value $J_{TH} > 0$ is a threshold parameter. Hence, we introduce J_{TH} to take into account measurement noise, as well as, high frequency switching in the CHB- nL converter. Regarding this parameter, the corresponding value can be set by running the system under a free-fault scenario such that

$$J_{TH} = \max_{no \text{ fault}, \forall t, p, j} |\hat{f}_{pj}^{DC}(t)|. \quad (11)$$

Therefore, fault detection incidence takes place as follows

$$\text{Fault Decision} = \begin{cases} \text{Fault,} & |r_{pj}| > 0 \\ \text{No Fault,} & |r_{pj}| = 0 \end{cases} \quad \forall j. \quad (12)$$

Once a fault is detected, the sign of the fault residuals r_{pj} is evaluated so that the faulty H-bridge is isolated.

4. SIMULATION RESULTS

In order to evaluate the OCF diagnosis strategies addressed in this work, a simulation of a 3-Phase APF based on a seven-levels cascaded H-bridge converter (CHB-7L) topology with $N = 3$ H-bridges, $p \in \{1, 2, 3\}$ and $j \in \{1, 2, 3\}$ is evaluated in the present section. The employed parameters during the evaluation stage: a source voltage of $127 V_{RMS}$ with $f_0 = 60$ Hz; a nonlinear load that includes a smoothing inductor of $L_0 = 0.1$ mH, DC capacitor $C_0 = 87 \mu\text{F}$ and output resistance $R_0 = 50 \Omega$; the APF has been designed with parameters $L = 5.0$ mH and $C = 2200 \mu\text{F}$. The discrete-controller scheme has been implemented in Simulink/MatLab, where a sampling frequency of $f_s = 40$ kHz is used. For this evaluation, the following cases are considered:

- i). A nominal (fault-free) scenario,
- ii). A single OCF in the first H-Bridge of phase 1,
- iii). Simultaneous (concurrent) OCFs in the first H-bridges of both phases 1&2.

Case i: Nominal (fault-free) scenario

Initially the 3-phase CHB-7 converter is evaluated working in closed-loop under the proposed scheme in a nominal condition. Figure 2 shows the time responses of the variables of interest. Notice that the compensated currents i_{Sp} are almost pure sinusoidal signals and are in-phase with the line voltages v_{Sp} despite the highly distorted load currents i_{0p} with $p \in \{1, 2, 3\}$. This implies that the APF injects appropriate currents i_p such that i_{Sp} have good tracking over the references i_{Sp}^* . In addition to the

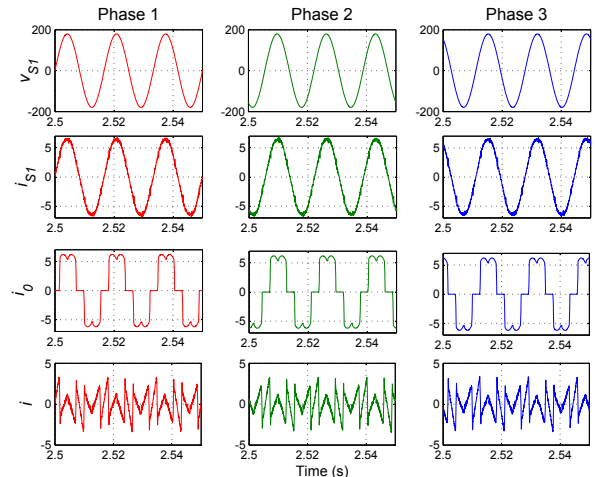


Fig. 2. The steady state responses of source voltages v_{Sp} , source currents i_{Sp} , load currents i_{0p} , injected currents i_p with $p \in \{1, 2, 3\}$.

above result, Fig. 3 illustrates that not only the tracking objective is accomplished, but also the regulation and balance objectives. It is shown that after a relatively short transient, the capacitor voltages v_{Cj} reach their reference values fixed at $V_d = 80$ V. However, the responses initially present an undershoot due to the presence of zeros in the right-half complex plane, as reported previously in the literature (Hooσσ and Bernstein, 2007).

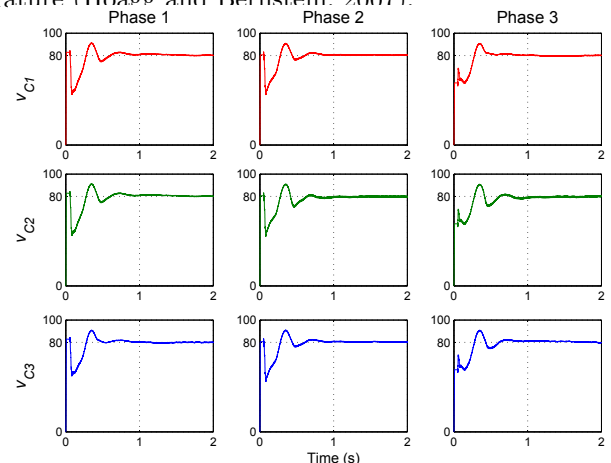


Fig. 3. The transient responses of capacitor voltages in all 3 H-bridges of the 3-phase APF.

After the steady-state is achieved, two cases of OCFs are considered, which are detailed in the two upcoming sections. For the detection criteria, the threshold value from expression (10) was chosen to be $J_{TH} = 0.10$, which was selected by observing the system under a fault-free and perturbation conditions, and measuring the peak value in the estimations.

Case ii: Single OCF Scenario

In this first scenario, the single OCF is induced at $t = 4$ s in the first H-bridge of the converter, specifically in switches (\bar{Q}_{11}, Q_{21}) . As a result, Fig. 4 illustrates how these faults are reflected in the dynamics of the capacitor voltages of the converter. The indicated signals are v_{Cpj}

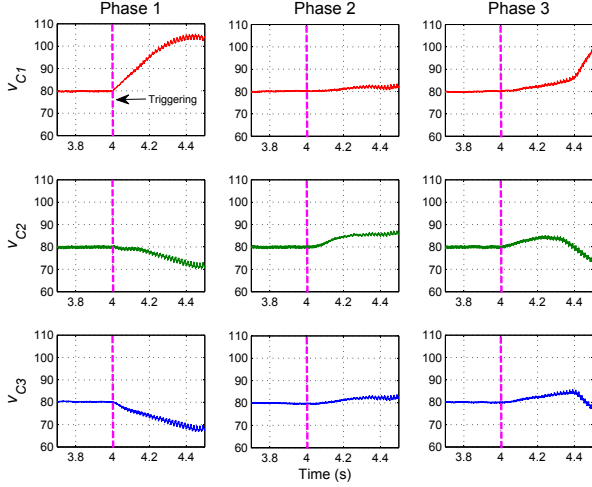


Fig. 4. Transient responses of capacitor voltages v_{Cpj} during single OCF scenarios in switches (\bar{Q}_{11}, Q_{21}) of phase 1.

with $j \in \{1, 2, 3\}$ of each phase $p \in \{1, 2, 3\}$. Observe that, once the OCF is invoked, these capacitor voltages diverge from their constant reference values reaffirming that the regulation and balance objectives are no longer achieved. Likewise, Fig. 5 characterizes the behavior of the estimated fault profiles during the above mentioned OCF scenario. At $t \approx 4.10$ ms the estimated fault profile \hat{f}_{11} exceeds the threshold value $J_{TH} = 0.10$. For this reason, H-Bridge 1 of phase 1 is identified as the faulty one. Notice that, the plots of \hat{f}_{1j} display a positive direction, this is because the faulty converter cannot generate the positive portion of the output voltage $u_{11}v_{C11}$ (section 3.1).

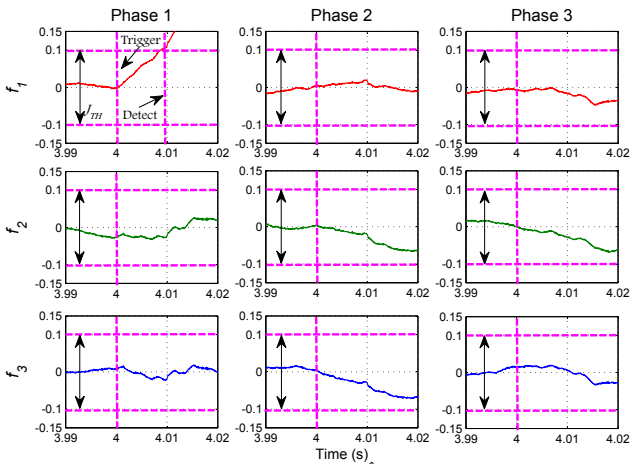


Fig. 5. Estimated fault profiles \hat{f}_{pj} during a single OCF in switches (\bar{Q}_{11}, Q_{21}) .

Case iii: Simultaneous OCF Scenarios

The results in this section validate the capability of the proposed FDI during simultaneous OCFs. Consequently, Figs. 6 and 7 show the propagations of the concurrent OCFs triggered in switches (\bar{Q}_{11}, Q_{21}) of phase 1&2 and

(Q_{11}, \bar{Q}_{21}) of phase 1&3, respectively. Observe that in this case, not only the fault profile \hat{f}_{11} exhibits the positive orientation, but also \hat{f}_{21} and \hat{f}_{31} . Hence, from these plots, it can be clearly seen that at $t \approx 4.10$ ms the fault profiles \hat{f}_{11} , \hat{f}_{21} and \hat{f}_{31} have exceeded the detection threshold at $J_{TH} = 0.10$. Therefore, the corresponding H-Bridges

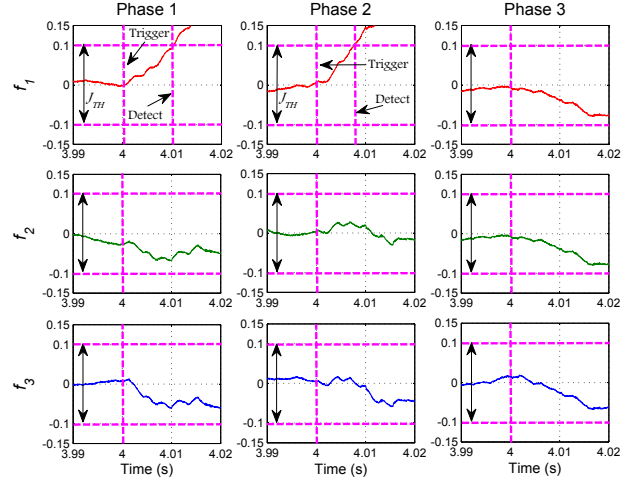


Fig. 6. Estimated fault profiles f_{pj} during concurrent OCFs in switches (\bar{Q}_{11}, Q_{21}) .

are characterized as the faulty ones, and as expected, the presence of fault in these H-Bridges is being pinpointed at exactly the same time $t \approx 4.10$ ms.

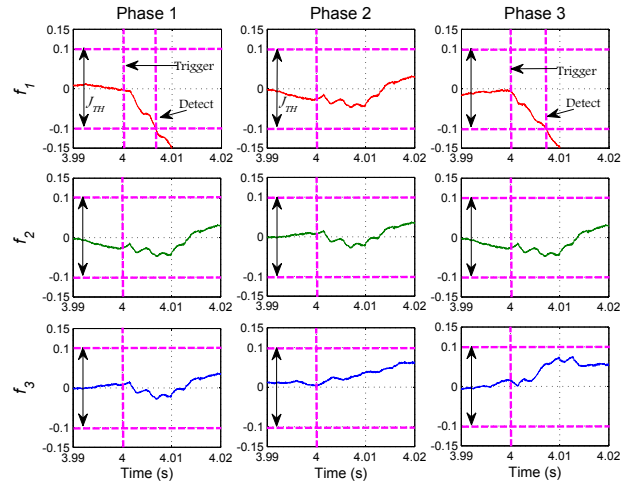


Fig. 7. Estimated fault profiles f_{pj} during concurrent OCFs in switches $(\bar{Q}_{11}, \bar{Q}_{31})$.

Last but not least, Fig. 8 validates the tolerance of the generated fault profiles \hat{f}_{pj} , in the presence of perturbations. This evaluation was conducted by changing the load resistance located in the diode bridge rectifier from 50 to 100 Ω and back to 50 Ω , at the interval: $t = 3.5 - 3.7$ s. As expected, the fault profiles remain unaltered.

CONCLUDING REMARKS

This work presented a generalized model-based fault diagnosis strategy for OCFs in the switching devices of a 3-phase CHB- nL converter used as shunt APF. In order to accomplish this goal, a bank of sliding-mode PI nonlinear observers per phase was suggested to estimate the fault

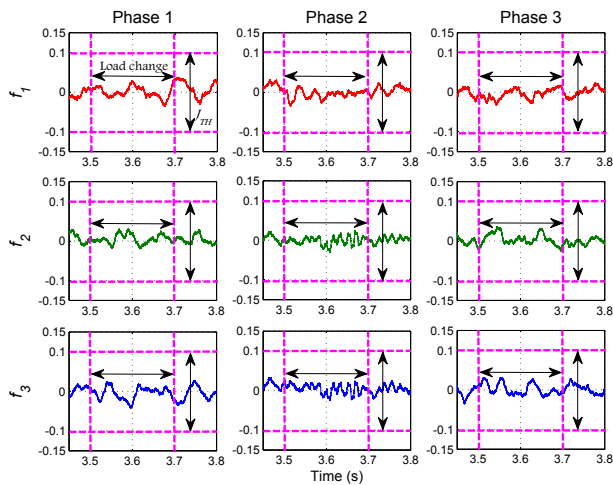


Fig. 8. Estimated fault profiles \hat{f}_{pj} during the step changes in the load resistance from 50 to 100 Ω and back to 50 Ω at the interval: $t = 3.5 - 3.7$ s.

profiles based on an additive fault model. These profiles were estimated to generate residuals that are independent of the operating point of the converter. As expected, the residuals were used for fault detection and isolation in the 3-phase CHB- n L APF.

An important property of the present research work is that the diagnosis media was carried out without the need of additional sensors, also the observers do not rely on the model parameters. To validate the ideas proposed in this work, a simulation study was conducted under single and concurrent OCF scenarios. During the evaluation, the proposed FDI methodology only required much less than a-cycle $t \approx 10$ ms, of the fundamental frequency f_0 throughout the fault scenarios.

REFERENCES

- A. A. Valdez-Fernández, P. R. Martínez-Rodríguez, G. Escobar, C. A. Limones-Pozos, and J. M. Sosa, A Model-Based Controller for the Cascade H-Bridge Multilevel Converter Used as a Shunt Active Filter. *IEEE Trans. Ind. Electron.*, 60:5019-5028, 2013.
- N. D. Marks, T. J. Summers, and R. E. Betz, Control of a 19 Level Cascaded H-bridge Multilevel Converter Photovoltaic System. *IEEE Energy Conversion Congress and Exposition (ECCE)*, 2265-22726, Pittsburgh, PA, Sept. 2014.
- C. D. Townsend, Y. Yu, G. Konstantinou, and V. G. Agelidis, Cascaded H-Bridge Multilevel PV Topology for Alleviation of Per-Phase Power Imbalances and Reduction of Second Harmonic Voltage Ripple. *IEEE Trans. Pow. Electron.*, 31:5574-5586, 2016.
- B. Mirafzal, Survey of Fault-Tolerance Techniques for Three-Phase Voltage Source Inverters. *IEEE Trans. Ind. Electron.*, 61:5192-5201, 2014.
- U.M. Choi, F. Blaabjerg, and K. B. Lee, Study and Handling Methods of Power IGBT Module Failures in Power Electronic Converter Systems. *IEEE Trans. Pow. Electron.*, 30:2517-2533, 2015.
- Z. Ji, J. Zhao, Y. Sun, X. Yao, and Z. Zhu, Fault-Tolerant Control of Cascaded H-Bridge Converters Using Double Zero-Sequence Voltage Injection and DC Voltage Optimization. *Journal of Power Electron.*, 14:946-956, 2014.
- C. Shu, C. Ya-Ting, Y. Tian-Jian, and W. Xun, A novel diagnostic technique for open-circuited faults of inverters based on output line-to-line voltage model. *IEEE Trans. Ind. Electron.*, 63:4412-4421, Jul. 2016.
- Q. T. An, L. Sun, and L. Z. Sun, Current residual vector-based openswitch fault diagnosis of inverters in PMSM drive systems. *IEEE Trans. Ind. Electron.*, 30:2814-2827, May. 2015.
- I. Jlassi, J. O. Estima, S.K. El Khil, N. M. Bellaaj, and A. J. M. Cardoso, Multiple open-circuit faults diagnosis in back-to-back converters of PMSG drives for wind turbine systems. *IEEE Trans. Ind. Electron.*, 30:2689-2702, May. 2015.
- K. O. Mtepele, D. U. Campos-Delgado, A. Valdez-Fernandez and J. A. Pecina-Sánchez, Fault tolerant controller for a generalized n-level CHB multilevel converter. *13th Int. Conf. on Power Electronics (CIEP)*, 75-80, Guanajuato, MX, 2016.
- K.O Mtepele, J. A. Pecina-Sánchez, D.U Campos-Delgado and A. A. Valdez-Fernández, Open Circuit Fault Diagnosis Strategy for a Generalized n -Levels CHB Multilevel Converter, *IFAC National Conference on Automatic Control (AMCA)*, 205-210, Queretaro, MX, 2016.
- J.A. Pecina-Sanchez, D.U. Campos-Delgado, D.R. Espinoza-Trejo, and E.R. Arce-Santana, Diagnosis of Open Switch Faults in Variable Speed Drives by Stator Current Analysis and Pattern Recognition. *IET Electric Pow. Appl.*, 7:509-522, 2013.
- R. Isermann, *Fault-Diagnosis Systems: An Introduction from Fault Detection to Fault Tolerance*. Springer, 2006.
- W. Perruquetti, and J.P. Barbot, *Sliding Mode Control In Engineering*. CRC Press, 2009. *IEEE Industry Appl. Magazine*, 22:27-37, April 2016.
- M. Alavi, D. Wang, and M. Luo, Model-based Diagnosis and Fault Tolerant Control for Multi-Level Inverters. *In Proc. IECON 2015*, 1548-1553, Yokohama, Japan, 2015.
- H.K. Khalil. *Nonlinear Systems*. 2nd Ed., Prentice Hall, 1996.
- S. Ouni, J. Rodriguez, *et al.*, A Fast and Simple Method to Detect Short Circuit Fault in Cascade H-Bridge Multilevel Inverter. *In Proc. ICIT 2015*, 866-871, Seville, Spain, 2015.
- A. A. Valdez-Fernández, K.O Mtepele, and D.U Campos-Delgado, A Generalized Model-Based Controller for the n-level CHB Multilevel Converter Used as a Shunt Active Filter. *IEEE Int. Autumn Meet. on Pow. Electron. and Comp. (ROPEC)*, Guerrero, MX, Nov. 2015.
- T. Wang, H. Xu, J. Han, H. Bouchikhi, and M. H. Benbouzid, Cascaded H-Bridge Multilevel Inverter System Fault Diagnosis Using a PCA and Multiclass Relevance Vector Machine Approach. *IEEE Trans. Pow. Electron.*, 30:7006-7018, 2015.
- J. B. Hoagg and D. S. Bernstein, Nonminimum Zeros-Much to do About Nothing. *IEEE Control Systems*, 27:45-57, 2007.
- S. Kouuro, M. Malinowski, K. Gopakumar, J. Pou, L. G. Franquelo, B. Wu, J. Rodriguez, M. A. Prez, and J. I. Leon Recent advances and industrial applications of multilevel converters. *IEEE Trans. Pow. Electron.*, 57:2553-2580, Aug. 2010.